Error analysis of a multi-cell groundwater model

Evangelos Rozos[a] and Demetris Koutsoyiannis[b]

Department of Water Resources and Environmental Engineering, School of Civil

Engineering, National Technical University of Athens, Athens, Heroon Polytechneiou

5, GR 15780 Zographou, Greece.

[a] Corresponding Author. E-mail address: rozos@itia.ntua.gr; Phone:

+30 210 7722841, Fax: +30 210 7722832

[b] E-mail address: dk@itia.ntua.gr; Phone: +30 210 7722831, Fax: +30 210 7722832

ABSTRACT

The basic advantages of the multi-cell groundwater models are the parsimony, speed, and simplicity that make them ideal for hydrological applications, particularly when data are insufficient and/or repeated simulations are needed. However, the multi-cell models, in their basic version, are conceptual models and their parameters do not have physical meaning. This disadvantage may be overcome by the Narasimhan & Witherspoon's integrated finite difference method, which, however, demands that the cells' geometry conforms to the equipotential and no-flow lines. This restriction cannot be strictly satisfied in every application. Particularly in transient conditions, a mesh with static geometry cannot conform constantly to the varying flow kinematics. In this study, we analyse the error when this restriction is not strictly satisfied and we identify the contribution of this error to the overall error of a multi-cell model. The

study is experimental based on a synthetic aquifer with characteristics carefully selected so as to be representative of real world situations, but obviously the results of these investigations cannot be generalized to every type of aquifer. Nonetheless these results indicate that the error due to non-conformity to the aforementioned restriction plays a minor role in the overall model error and that the overall error of the multi-cell models with conditionally designed cells is comparable to the error of finite difference models with much denser discretization. Therefore the multi-cell models should be considered as an alternative option, especially in the cases where a discretization with a flexible mesh is indicated or in the cases where repeated model runs are required.

1. INTRODUCTION

Multi-cell models are multi-dimensional extensions of the completely mixed reactor model of chemical engineering (e.g., Aris, 1994). Key properties of these models are: (i) that the density of mesh nodes can be easily adjusted to fit irregular geometries efficiently with polygonal cells and (ii) that the setting up of the relevant equations is straightforward. These two advantages, in combination with the assumption of steady flow, have made the multi-cell models popular in water quality modelling such as in the multi-box simulation method of lake water quality (Thomann & Mueller, 1987).

Multi-cell models are also applied, to a lesser extent, in groundwater hydrological applications. Bear (1979) suggests using streamlines as parts of cell boundaries, which is more or less the concept behind the graphical method of flow-nets. Flow-nets have been introduced since the beginning of 20th century by Philipp Forchheimer to calculate the leakages under dams (Ettema, 2006). Narasimhan & Witherspoon (1976), building on the work of others, especially in the field of heat transfer (MacNeal, 1953; Dusinberre, 1961; Edwards 1972), have developed the method of

Integrated Finite Difference (IFD) that can be also considered as the mathematical background of the graphical flow-nets method. A particular requirement of this method is that it strictly demands continuous adjustment of the mesh geometry to the flow kinematics, so that the cell boundaries are equipotentials or no-flow lines. Narasimhan & Witherspoon (1976) express this (in a not so explicit fashion) as follows: "*For maximum accuracy, interfaces between elements should be perpendicular to the line joining the two nodal points and intersect that line at an appropriate mean position (arithmetic mean of nondivergent coordinates, log mean of cylindrical radii, or geometric mean of spherical radii). This ideal situation may be difficult to achieve in practice but should be approximated as closely as possible.*" The application tests of Narasimhan & Witherspoon (1976) are chosen such that essentially the situation is ideal; however, in most real-world problems the situation is far from ideal.

Narasimhan & Witherspoon's study proves that the multi-cell models, with appropriately designed cells, are able of functioning as physically based models in steady state conditions. However, in transient conditions, a continuous adjustment of cells' geometry to the flow kinematics is required. This is a very constraining requirement, which is likely the main reason why the multi-cell models have not been used widely for flow simulations.

The overall simplicity of the multi-cell models has motivated us to explore their application in transient groundwater simulations in addition to steady flow conditions, where the latter serves as reference basis for comparison. We wish to identify whether and under what conditions this method could be an appealing alternative when the data are sparse, and thus elaborate methods may not be warranted, or when repeated model runs must be made in the context of complex water resources management

simulations, where computing efficiency is important. To this end, we examined three type of errors related with the multi-cell models: (1) the error due to inexact conformity of the cells' geometry to the flow kinematics, (2) the truncation error and (3) the representational error; the last two errors are common in every distributed (hydrogeologic) model. We investigate the dependence of these three errors on the density and on the geometry of a multi-cell discretization mesh.

The investigation is not based on a classical mathematical analysis but rather on experiments performed on a synthetic aquifer with a stochastic hydraulic conductivity field that resembles field conditions. For this reason, and though the characteristics of this aquifer were carefully selected to be representative of typical conditions met in groundwater applications, the conclusions of this study cannot be applied to every aquifer transient simulation (with arbitrary temporal and spatial distribution of stresses and boundary conditions). Rather they can serve as a reminder of the existence of alternative modelling methods that can be advantageous in some applications.

The results of a coarse multi-cell representation are compared against those of a typical detailed representation using MODFLOW. The coarse multi-cell model used in this study is the 3dkflow model (Rozos et al., 2004; Rozos and Koutsoyiannis, 2006). 3dkflow is a model that supports meshes with arbitrary geometry i.e. the cells can be rectangular or irregularly shaped. 3dkflow is using a hydraulic analogous for simulating the water flow. This analogous is a network of interconnected tanks through water pipes. All aquifer properties and processes related with storage are simulated by the tanks whereas all properties and processes related with water transfer are simulated by the pipes.

The paper begins with an introduction to the Narasimhan & Witherspoon's method. This method is a simplification (enabled by the flow-nets-like discretization) of the widely used nowadays Finite Volume Method (FVM) (Carrera, 2008). For this reason in this study we chose a term that simultaneously denotes the method's relation with the FVM and indicates its distinctiveness. This new term is Finite Volume Method with Simplified Integration (FVMSI) used in this study in the context of the flow-nets-like discretization required by the multi-cell models to function as physically based models.

Afterwards we present two case studies. In the first case study, four FVMSI meshes are used to simulate a synthetic aquifer under steady state conditions. Reference simulations are used to derive the overall error of the simulations with each FVMSI mesh. The second case study concerns the flow simulation in the synthetic aquifer under transient conditions, with the four FVMSI meshes, and the comparison of their accuracy with the accuracy achieved using the Finite Difference Method (FDM) with four grids.

The paper closes with the summary of the methods and the findings of this study.

2. MULTI-CELL MODELS AND FVM

2.1 Finite Volume Method

The differential equation of the groundwater movement in a confined anisotropic aquifer is (Bear, 1979):

$$\nabla \cdot \mathbf{K} \, \text{grad} \, h + G = \text{SS} \, \frac{\partial h}{\partial t} \tag{1}$$

where h is the hydraulic head [L], $\mathbf{K}$ is the tensor of the hydraulic conductivity [L T^{-1}], G is the external stress [T^{-1}], and SS the specific storage [L^{-1}]. If the coordinate

system coincides with the principal axes of anisotropy, then the off-diagonals terms of the tensor **K** are zero.

When the space derivatives of the hydraulic head in equation (1) are approximated with finite differences, it is common to discretize the domain on a rectangular grid. To avoid this restriction, an alternative technique is used in the FVM. Equation (1) is integrated with respect to the volume V of the discretization cell:

$$\int_V (\nabla \cdot \mathbf{K} \text{ grad } h + G) \, dV = \frac{\partial}{\partial t} \int_V \text{SS } h \, dV \tag{2}$$

According to the divergence theorem of Gauss, and assuming that SS is constant and G and h are space invariant inside the cell, equation (2) is written as (Knabner and Angermann, 2003):

$$\int_S \mathbf{K} \text{ grad } h \cdot \mathbf{n} \, d\mathbf{S} + G \, V = \text{SS } V \frac{\partial h}{\partial t} \tag{3}$$

The surface integral at the left side of equation (3) is the total discharge crossing the surface S that surrounds the volume V, and **n** is the unit vector normal to a surface element d**S** (positive outwards). The application of equation (3) to all cells of the grid, results in a system of linear equations. The hydraulic head in the centres of the cells is obtained from the solution of this system.

2.2 Simplified integration

The surface integral in the left side of equation (3) cannot be calculated analytically in every case, so numerical methods (e.g., the trapezoidal rule or Gauss integration) must be used. Several studies have been conducted on these numerical methods to achieve better accuracy with simpler algorithms (Wenneker et al., 2000; Moroney and Turner, 2004). A methodology that simplifies the calculation of this surface integral was implemented in the present work.

We focus our study on isotropic aquifers (anisotropic aquifers can be transformed to isotropic with the appropriate mapping; Strack, 1999). In this case **K** reduces to a scalar K. A condition that simplifies the calculation of the integral in (3) is met when the edges of the discretization cells are equipotential lines or no-flow lines (hereafter referred as the 1st FVMSI condition). In this case, the product grad $h \cdot \mathbf{n}$ along the perimeter of each cell is equal to $\pm|$grad $h |$ ($|$grad $h | = 0$ on no-flow edges). Consequently, the calculation of the surface integral is reduced to a simple summation of terms of Darcian fluxes.

Indicated position for Figure 1

In the example shown in Figure 1, the cell m is surrounded by N neighbouring cells. By substituting finite difference ratios for the time derivative and the $\pm|$grad $h |$, equation (3) for cell m is written as follows:

$$G_m\, V_m + \sum_{n=1}^{N} K_{mn} \frac{h_n - h_m}{D_{mn}} A_{mn} = \mathrm{SS}_m\, V_m \frac{\Delta h_m}{\Delta t} \qquad (4)$$

where D_{mn} is the distance between the centres of cells m and n [L], A_{mn} the common surface between the cells m and n [L^2], K_{mn} the conductivity between the cells m and n [L T^{-1}], G_m the stress on the cell m [T^{-1}], V_m the volume of cell m [L^3], and SS$_m$ the specific storage of cell m [L^{-1}].

It is reminded that the specific storage SS$_m$ equals the storage coefficient divided by the thickness of the aquifer (s_m/B) and is suitable for describing only confined aquifers. In an unconfined (phreatic) aquifer, the equivalent quantity is the specific yield divided by the hydraulic head i.e. SY$_m/h_m$. Furthermore, in an unconfined aquifer, V_m is not the volume of cell m but the volume of the saturated part of cell m, i.e., $V_m = E_m\, h_m$, where E_m is the surface area of cell m. Hence, in the case of an unconfined aquifer, equation (4) is written as:

$$G_m V_m + \sum_{n=1}^{N} K_{mn} \frac{h_n - h_m}{D_{mn}} A_{mn} = SY_m E_m \frac{\Delta h_m}{\Delta t} \qquad (5)$$

This equation is non-linear (A_{mn} depends on h_m and h_n); a linearization technique is the most convenient approach to solve it. The simplest linearization is to consider that A_{mn} is constant between stress periods. More elaborate techniques are described by Upadhayaya and Chauhan (2001).

In the two previous equations, $|\text{grad } h|$ between cells m and n is approximated by $(h_n - h_m)/D_{mn}$. This approach implies that the line linking the centres of cells m and n is perpendicular to their common edge. This requirement constitutes the 2nd FVMSI condition, which is not necessary to hold for cells separated by no-flow lines.

If FVMSI is applied in transient conditions, the mesh geometry can be designed so that the above two conditions are satisfied at a representative state (e.g., a steady-state approximation assuming time average stresses, the median state over the whole simulation period, or the state at the middle of the simulation period).

The FVMSI is implemented in the 3dkflow model (Rozos et al., 2004; Rozos and Koutsoyiannis, 2006). This model uses a hydraulic analogue with two components (pipes and reservoirs) that correspond to the (transport) flow and storage properties of the aquifer (groundwater mass). All types of stresses are simulated with appropriate changes in the water level of the reservoirs and all boundary conditions are modelled with properly selected reservoir characteristics (for example, a spring is modelled using a spring-type reservoir, i.e. a reservoir with very large base).

2.3 Errors of the FVMSI multi-cell model

In a typical application with steady state conditions, the conformity of the mesh geometry with the FVMSI conditions improves with the discretization density. If a

coarse mesh is used to discretize the flow domain, the edges of the cells can be drawn on the equipotential lines (conformity to the 1st FVMSI condition), but not all lines connecting the gravity centres of neighbouring cells will be perpendicular to their common edge (non-conformity to the 2nd FVMSI condition). In transient conditions the varying flow kinematics renders impossible the conformity of the mesh geometry with the two FVMSI conditions regardless of the discretization density.

The multi-cell models' overall error, apart from the error due to non-conformity, includes also two more types of error, which are common in every distributed hydrogeologic model. These are the truncation error and the representational error.

A formal basis for developing finite difference approximation to derivatives is through the use of Taylor series expansion. The common methodology in numerical methods is to keep only the first two or three terms of these series and consider the truncated terms as the error of this approximation. The truncation error depends on the distance between the discretisation nodes. If the distance between nodes is Δx, then the leading term of the truncation error of the approximation of the second spatial derivative at x_0 is $-\Delta x^2/12 \, h''''(x_0)$, where $h''''(x_0)$ is the value of the fourth spatial derivative of the hydraulic head at x_0 (Özişik, 1994). Therefore the truncation error is reduced with increased discretization density.

The representational error stems from the inefficient representation of the aquifer boundary conditions, stresses and properties because of the insufficient spatial discretization. According to Lal (2000) this error is $7.8 \, (k_i \, \Delta x)^2$, where k_i is the wave number of the i frequency component of the solution. In the inverse problem, the representational error is strongly influenced by the aquifer parameterization, a procedure that attempts to establish a mapping between the spatial variation of the aquifer properties (hydraulic conductivity for example) and a, small in number, set of

parameters. This procedure is essential since it both reduces the number of calibrated parameters and increases the stability of the solution (Stallman, 1956).

In summary, both the truncation and the representational error are reduced with the increase of the discretization density. In the following case studies we try to identify the influence of the discretization density on the non-conformity error and the significance of each of the three errors on the overall error of a FVMSI multi-cell model.

3. MULTI-CELL MODELS' ERROR IN STEADY STATE CONDITIONS

3.1 Description

In a first case study, the errors of four FVMSI meshes with 150, 73, 37 and 10 cells are investigated in a synthetic non-homogenous aquifer under steady state conditions. The synthetic aquifer is appropriately parameterized, individually for each mesh, to minimize the influence of the representational error. The deviations from reference values, obtained from high-resolution MODFLOW simulations, give the estimations of the multi-cell models' overall error.

3.2 Generation of the synthetic conductivities field

The synthetic values of conductivity are produced by a stochastic model that is based on the extension in two dimensions of the Symmetric Moving Average algorithmic scheme (Koutsoyiannis, 2000; Theodoratos, 2004), which is appropriate to simulate fields with long-range dependence (Hurst effect). The function that gives the process in a discrete two-dimensional space is:

$$Z(i,j) = \sum_{m=-q}^{q} \sum_{n=-q}^{q} \alpha(m,n)\, U(i-m, j-n) \quad (6)$$

where i, j are the coordinates of element (i, j), $U(i, j)$ random innovations ($\mathrm{E}[U(i, j)] =$ 0, $\mathrm{Var}[U(i, j)] = 1$) and $\alpha(m, n)$ is a matrix of weights such that $\alpha(-m, n) = \alpha(-m, -n) = \alpha(m, -n) = \alpha(m, n)$, with m and n ranging from $-q$ to q. The weights are properly calculated to confer desirable statistical characteristics to the process, i.e., Hurst coefficient H and variance γ_0. For a positively autocorrelated field, H ranges between 0.5 and 1 and is related to the correlation length of the geostatistical models. The stochastic model was applied with $q = 25$, $H = 0.9$ and $\gamma_0 = 0.01$ to produce 100×100 discrete values of conductivity with a lognormal distribution. For this reason, even such a low variance coefficient is enough to produce a wide range of variation of the conductivities. The Hurst coefficient was deliberately chosen to have a high value (close to 1), to ensure the presence of large areas with similar conductivities. The constant q was chosen large enough, to take into account all the significant weights $a(m,n)$. Figure 2(a) shows the produced field (panels (b), (c) and (d) of this figure are discussed in section 4.3).

Indicated position for Figure 2

3.3 Hypothetic aquifer with steady state stresses

The hypothetic aquifer is square in plan view, with side length equal to 50 km. Square shaped aquifer was selected to facilitate the FDM model setup. An irregularly shaped aquifer would most certainly result in an increase of the representational error of the FDM. On the contrary, the representational error of the FVMSI, which is able of using irregularly shaped cells for discretization, would not increase. Therefore the square shaped aquifer, used here for convenience, benefits only the reference method (FDM).

The stresses applied on this hypothetic aquifer are a uniform constant recharge (2.6 mm/d) and a series of constant-strength injection wells (total recharge 25 m^3/s)

located on the lower right side. The aquifer discharges through a series of drains located in the middle section of the upper side. The aquifer boundary conditions, the series of wells and the drains are displayed in Figure 3. The aquifer is confined and its thickness is 100 m.

<div align="center">**Indicated position for Figure 3**</div>

3.4 Discretization of the synthetic aquifer with four FVMSI meshes

Four FVMSI meshes (with 150, 73, 37 and 10 cells) are used to discretize the flow domain (Figure 4). The geometry of these meshes is derived from the equipotential lines of the hydraulic head (contours). Different contour interval is used for each FVMSI mesh, i.e. contour interval of 10, 20, 40 and 80 m for the meshes with 150, 73, 37 and 10 cells. The equipotential lines are obtained from the simulation of the original synthetic aquifer with MODFLOW.

<div align="center">**Indicated position for Figure 4**</div>

In all four meshes, the cells closest to the drains are connected with a special spring-type cell, whereas the cell at the right-bottom corner receives a supplementary recharge that corresponds to the injection wells.

In this case study we are investigating the influence of the truncation and the non-conformity error on the overall error. To eliminate the representational error related to the spatial variation of the aquifer properties, four parameterizations of the original synthetic aquifer are used to derive the reference values of the four FVMSI meshes. These parameterizations are produced with four zonations of the original synthetic aquifer with 150, 73, 37 and 10 homogeneous zones. The conductivity of each zone, which is also the conductivity value of the corresponding FVMSI cell, is derived with aggregation (arithmetic mean) of the synthetic field values (of the original synthetic aquifer) inside this zone. Two sets of reference values are obtained with MODFLOW

(simulates the four parameterized aquifers) using a 100×100 discretization grid. The first set is recorded at the MODFLOW cells closest to the gravity centres of the FMVSI cells whereas the second set is the arithmetic mean of the hydraulic head in MODFLOW cells grouped by the FVMSI cells.

3.5 Results

The four FVMSI meshes are used by 3dkflow to simulate the corresponding four parameterized aquifers. The deviations between the 3dfklow simulations and the reference values give the overall error for the FVMSI meshes.

The error of the FVMSI meshes is displayed in Figure 5. Vertical dashed lines divide the first three charts of this figure (corresponding to meshes with 150, 73 and 37 cells) into six sections and the last chart (corresponding to the mesh with 10 cells) into three sections. These sections correspond to the FVMSI columns of cells that run from the lower to the upper edge of the aquifer (first column marked in Figure 4(a) is the column that corresponds to the first section of the chart in Figure 5(a)). The values at the beginning of each section correspond to the cells closer to the lower edge of the aquifer whereas the values closer to the end of each section correspond to the FVMSI cells closer to the drains.

Figure 5 indicates that the discretisation with 150 cells exhibits the largest overall error. A comparison between the four charts of Figure 5 indicates also that the overall error gets increasingly smaller from the mesh with 150 cells to the mesh with 37 cells, which is counterintuitive. The mesh with 10 cells has the second largest overall error. Finally, in all meshes the overall error tends to be lower at the cells closer to the drains.

Indicated position for Figure 5

In this case study the reference values are derived from the corresponding parameterized aquifers, hence the representational error is almost eliminated. Therefore, in this case, the overall error includes the error due to non-conformity to the 2nd FVMSI conditions and the truncation error.

The increase of the discretization density results in the decrease of the truncation error. However, the mesh with the densest discretization (150 cells) exhibits the largest overall error of the simulated hydraulic head (RMS = 8.25 m). This means that this discretization introduces the largest non-conformity error. An examination of Figure 4 reveals that the unidirectional increase of the discretization density results in elongated cells that do not conform to the 2nd FVMSI condition.

The overall error declines with the reduction of the resolution; the mesh with 37 cells has the lowest RMS error (3.54 m). The overall error of the mesh with 10 cells is the second largest error (6.60 m). This increase is attributed to the truncation error, which plays more important role at the coarser discretizations.

In all four meshes, the overall error is lower at the cells closer to the drains. This happens because in those boundary conditions the hydraulic head is constant and known. This information is transmitted to the neighbouring cells, improving the accuracy of simulated hydraulic head there.

4. MULTI-CELL MODELS' ERROR IN TRANSIENT CONDITIONS

4.1 Description

The second case study is closer to a typical hydrogeological application. The synthetic aquifer of the first case study is simulated under transient conditions to produce synthetic observations. The simulation is performed with MODFLOW on a 100×100

discretization grid. These observations are used for the calibration of the conductivities of the four multicell models with FVMSI meshes.

The synthetic observations are also used for the calibration of the conductivities of four FDM models. The accuracy of the simulations with the FVMSI models is compared against the accuracy of the simulations with the FDM models in terms of the simulated hydraulic heads, drains discharge and calibrated conductivities.

4.2 Hypothetic aquifer with transient stresses

The transient simulation includes 120 monthly stress periods. Uniform recharge is applied to the aquifer following the temporal pattern of six months of constant recharge equal to 5.20 mm/d and six months of zero recharge. The total recharge of the wells is switching from 50 to 0 m^3/s every six months. This type of stress, apart from being common in many real applications (infiltrating water from mountainous regions), also considerably alters the shape of the equipotential lines close to the wells (to ensure non-conformity to the FVMSI conditions and investigate the implications). The specific storage of the aquifer is assumed equal to 0.001 m^{-1}.

4.3 Discretization with four different FDM grids and parameterization of the synthetic aquifer with six zones

The synthetic aquifer is parameterized using six zones of homogeneous conductivity that correspond to six conductivity classes. The choice of the number and range of the classes, decided after a preliminary investigation, ensures the fewest parameters with the smallest possible introduced error (the simulation of the aquifer by applying the median values of the six classes to the corresponding cells of the six zones gave virtually the same results with the simulation of the aquifer using the 100×100 conductivity values from the stochastic model).

To construct a comparison base, three new grids with lower discretizations (50×50, 20×20 and 12×12) are produced. These are derived through spatial aggregation (based on arithmetic mean) of the synthetic 100×100 field. Again, the cells of these three discretizations are classified into 6 zones according to the same classes. This results in four grids (100×100, 50×50, 20×20 and 12×12) with parameterizations of six zones. The parameterization of the four FDM grids is presented in Figure 2.

Hydraulic head values from the simulation of the original synthetic aquifer are recorded on a hypothetical 8×8 observation-grid. These observations are used in the calibrations of the conductivities of the four FDM grids. The upper-most left node of the observation grid corresponds to the cell (8,8) and the lower-most right node to the cell (92,92) of the 100×100 synthetic field (see Figure 3).

4.4 Calibration and simulation of the synthetic aquifer with the four FDM grids

The same stresses, boundary conditions and porosity are applied to all four FDM grids. The objective function is the Root Mean Square (RMS) of the differences between the simulated head values and the corresponding values of the observation grid. The six conductivity parameters are calibrated with the MODFLOW2000 internal optimization algorithm (Hill et al., 2000).

4.5 Parameterization of the synthetic aquifer with the four FVMSI meshes

The FVMSI cells are grouped into classes according to the average class of the corresponding cells of the 100×100 grid. The group to which each FVMSI cell belongs is marked with different colour in Figure 4. The cells of the meshes with 150 and 73 cells are grouped into six classes. The cells of the mesh with 37 cells are grouped into four classes and the cells of the mesh with 10 cells are grouped into three

16

classes (the number of classes that can be distinguished is lower at the coarser discretizations because of the elimination of the extreme values by the aggregation).

4.6 Calibration and simulation of the synthetic aquifer with four different FVMSI meshes

The same uniform recharge, injecting scheme and porosity used in the FDM grids are also applied to the four FVMSI meshes. The objective function of the calibration procedure is again the RMS of the differences between the simulated hydraulic heads and the synthetic observations.

The locations where these observations are recorded are the cells of the 100×100 grid closest to the gravity centres of the 3dkflow cells. The reason why we used values from single cells in our comparisons, instead of aggregating, is because we wanted to test the multi-cell model under operational conditions. The usual situation in real applications is to have very limited number (not enough for interpolations) of available localized measurements. In such cases, there is no other option than to compare the localized measurements (represented by the values from single cells in our synthetic case study) directly against the simulated hydraulic heads on the gravity centres of the closest cells (with careful design, the measurement locations can coincide with the gravity centres of the discretization cells).

The conductivity parameters are calibrated with the Shuffled Complex Evolution algorithm (Duan et al., 1992). This is a very powerful algorithm, which is not trapped to local minima but requires many iterations to converge.

4.7 Results

The average RMS errors of the simulated hydraulic heads (hereafter referred as HRMS) and the RMS errors of the drains' discharge (QRMS) for MODFLOW with grids 100×100, 50×50, 20×20 and 12×12, and for 3dkflow with 150, 73, 37 and 10

cells are shown in the Figure 6 and Figure 7 respectively. These figures display also the trend line of the four (n, HRMS) and the four (n, QRMS) MODFLOW pairs, where n the number of the discretization cells.

Indicated position for Figure 6

Indicated position for Figure 7

The maximum hydraulic head error (including the hydraulic head simulated in every cell for the whole simulation period) and the maximum discharge error for MODFLOW and 3dkflow are shown in Table 1.

Indicated position for Table 1.

The deviations of the calibrated conductivities with the four FDM grids from the reference values (medians of the conductivity classes) are displayed in Figure 8. This figure suggests that only the discretization with 100×100 gives satisfactory estimations for all 6 parameters.

Indicated position for Figure 8

The deviations of the calibrated conductivities with the four FVMSI grids from the reference values are displayed in Figure 9. This figure suggests that only the mesh with 73 cells gives satisfactory estimations for all 6 parameters. The mesh with 37 cells gives good estimates for the four calibrated parameters.

Indicated position for Figure 9

In this case study, the simulation of the original synthetic aquifer under transient conditions provides the reference values for the calibration of the four FVMSI meshes. For these calibrations to be successful, the spatial variation of the aquifer hydraulic conductivity should be reproduced. Therefore, the accuracy of the representation of the aquifer properties, which increases with the discretization density, is influencing the simulations error. According to Figure 6, Figure 7 and

18

Table 1, the simulation accuracy of the mesh with 150 cells is lower than the accuracy of the mesh with 73 cells (better QRMS, slightly worse HRMS but much worse maximum error). This happens because of the increased non-conformity error of the denser discretization. Likewise, the reliability of the estimated parameters is decreased in the mesh with 150 cells. Therefore, again as in the previous case study, there is an optimum discretization, which in our case study is the mesh with 73 cells (if the reliability of the simulated hydraulic head and estimated parameters is the most important issue) or the mesh with 150 cells (if the simulation accuracy of the discharge is the most important issue).

Figure 6, Figure 7 and Table 1 demonstrate that the errors of the FDM evolve quite smoothly with the discretization density and fit well with a power-law trend line. This is not the case for the overall errors of the FVMSI multi-cell models, which evolve less predictably with the number of cells. This happens both because of the interaction of the three error source mechanisms and of the effect of the different number of observations used in optimizations (discussed in the next paragraph). In any case, the FVMSI meshes achieved simulation accuracy equivalent with FDM discretizations with ten times more cells concerning the hydraulic head and even higher accuracy concerning the discharge. This improved accuracy is attributed to the reduction of the representational error in the former. The FVMSI meshes achieve this reduction for two reasons. First, the mesh is flexible and can be easily adapted to irregularly shaped aquifer (this is not the case in our study, where a square-shaped aquifer is used). Second, the cell edges are drawn on the equipotential lines, which get denser in areas with low conductivity and vice versa. Therefore, the mesh geometry itself incorporates a representation of the spatial variation of the aquifer properties, which relaxes the need for high resolution. The mesh geometry helps also to achieve

an efficient parameterization for the inverse problem. Actually the mesh itself is also a kind of parameterization since its form reflects the variation of the flow properties.

It must be noted here that different numbers of observations are used in the calibrations of the multi-cell models with FVMSI meshes and the calibrations of the FDM models. In all four FDM models, 64 hydraulic head time series are used as observations. On the other hand, the number of time series used in the multi-cell models equals the number of cells of the FVMSI meshes. We chose this method to avoid any kind of interpolation or integration, which would be another source of error. The increase of the number of the observations helps to estimate more reliably the model parameters, but also intensifies the detection of the model errors. Therefore, the actual relative accuracy (compared with the FDM) of the multi-cell models with 150 and 73 cells can be even higher than that indicated in the comparisons of Figure 6 (of course, the opposite holds true for the multi-cell models with 37 and 10 cells).

A final experiment was conducted using the FVMSI mesh with 10 cells. This time, a dedicated conductivity parameter was used for each cell (10 parameters in total). The optimization achieved very good accuracy with HRMS=0.79 m and QRMS equal to 0.89 m^3/s (Figure 6 and Figure 7), but the calibrated parameters deviate significantly from the reference values. Since the calibrated parameters are not related with the properties of the synthetic aquifer this is a kind of a conceptual model. Nevertheless, it must be noted that the topology of this model is derived from the physical properties of the aquifer, which is an advantage over other types of conceptual models, where the model topology is defined arbitrarily.

6. SUMMARY AND CONCLUSIONS

In this study the error of the multi-cell models with conditionally designed meshes is examined in steady state and transient groundwater flow conditions. These models are

based on the Finite Volume Method with Simplified Integration, which dictates that the mesh geometry should conform to the flow geometry. To investigate the implications of this condition, a synthetic non-homogeneous aquifer was employed. The stresses (both steady state and transient) and boundary conditions were chosen to be representative of a typical hydrogeological application. The absence of any distinct characteristic (apart from the aquifer square shape, which favours the reference method i.e. FDM) enables drawing the following conclusions:

- The FVMSI meshes help to reduce the representational error because the mesh geometry incorporates information about the spatial variability of the aquifer properties. The smaller the contour interval of the equipotential lines used to produce the FVMSI mesh, the more detailed is the information incorporated into the mesh.

- A unidirectional increase of the discretization density decreases the representational and the truncation error but increases the non-conformity error.

- In our case study, the accuracy of the simulated hydraulic head and discharge with an FVMSI mesh in transient conditions is equivalent to the accuracy of an FDM model with much denser discretization grid (discretization with almost one order of magnitude more cells). This holds true also for the reliability of the estimated parameters.

- An FVMSI mesh with very few cells can be used as a conceptual model. Although the parameters of this model might be loosely related with the actual aquifer properties, its topology is derived from the flow properties, which is an advantage over other conceptual models where the topology is arbitrary.

- Finally, the FVMSI meshes are flexible and thus they adapt more easily to irregularly shaped aquifers.

Advances in computer technology have indeed endowed PCs with significant computing power, and this often makes the need for "fast and simple" solutions not a pressing issue, if one is interested in occasionally solving a particular flow problem. However, the inherent virtues of parsimony and efficiency become desirable in engineering applications in which large, complex codes must be executed repeatedly. This is where multi-cell models with FVMSI meshes may become (under the conditions described above) a good alternative option, since they combine increased speed, due to limited number of cells, with a very good accuracy. However these models require a careful preliminary study to identify the optimum discretization density (a case study facing all these issues has been presented by Efstratiadis et al., 2008).

REFERENCES

Aris, R. (1994) Mathematical Modelling Techniques, Courier Dover Publications.

Bear, J. (1979) Hydraulics of Groundwater. McGraw-Hill, New York, USA.

Carrera, J. (2008), Groundwater: Modeling Using Numerical Methods in Encyclopedia of Water Science, ed. S. W. Trimble, Edition: 2, CRC Press, 2007, p. 450.

Dusinberre, G . M. (1961) Heat Transfer Calculations by Finite Differences, International Textbooks, Scranton, Pa.

Duan Q., S. Sorooshian and V. Gupta (1992), Effective and efficient global
optimization for conceptual rainfall-runoff models. Water Resources Research,
28(4), pp. 1015-1031.

Edwards,A . L. (1972) Trump:A Computer Program for Transient and Steady State
Temperature Distributions in Multidimensional Systems, National Technical
Information Service, National Bureau of Standards, Springfield, Va.

Efstratiadis, A., I. Nalbantis, A. Koukouvinos, E. Rozos, and D. Koutsoyiannis,
HYDROGEIOS: A semi-distributed GIS-based hydrological model for modified
river basins, Hydrology and Earth System Sciences, 12, 989–1006, 2008.

Ettema R. (2006), Hunter Rouse—His Work in Retrospect, J. Hydr. Engrg. Volume
132, Issue 12, pp. 1248-1258.

Hill M. C., E. R. Banta, A. W. Harbaugh and E. R. Anderman (2000), MODFLOW-
2000, the U.S. geological survey modular ground-water model user guide to the
observation, sensitivity, and parameter-estimation processes and three
postprocessing programs, Denver.

Knabner, P. and L. Angermann (2003), Numerical methods for elliptic and parabolic
partial differential equations, Springer, New York, pp. 256-261

Koutsoyiannis, D. (2000) A generalized mathematical framework for stochastic
simulation and forecast of hydrologic time series. Water Resources Research, 36(6),
pp. 1519-1533.

Lal, A.M.W. (2000) Numerical errors in groundwater and overland flow models,
36(5), pp. 1237-1248.

MacNeal, R. H. (1953) An asymmetric finite difference network, Quart. Appl. Math.,
2, pp. 295-310.

Moroney T. J. and I. W. Turner (2004), A new finite volume method incorporating radial basis functions for simulating diffusion. The 12th Biennial Computational Techniques and Applications Conference, Melbourne.

Narasimhan, T.N. and P.A. Witherspoon (1976), An Integrated Finite Difference Method for Analyzing Fluid Flow in Porous Media. WRR, 12(1), pp. 57-64.

Özişik N. (1994) Finite Difference Methods in Heat Transfer, CRC Press, p. 40.

Rozos, E. and D. Koutsoyiannis (2006), A multicell karstic aquifer model with alternative flow equations, Journal of Hydrology, 325(1-4), pp. 340-355.

Rozos, E., A. Efstratiadis, I. Nalbantis and D. Koutsoyiannis (2004), Calibration of a semi-distributed model for conjunctive simulation of surface and groundwater flows, Hydrological Sciences Journal, 49(5), pp. 819-842.

Stallman, R. W. (1956) Numerical analysis of regional water levels to define aquifer hydrology, EOS Trans. AGU, 37(4).

Strack, O. D. L. (1999) Groundwater Mechanics, Prentice-Hall Minneapolis, pp. 211-215.

Theodoratos N. (2004) Stochastic simulation of two-dimensional random fields with preservation of persistence, thesis, Department of Water Resources, Hydraulic and Maritime Engineering - National Technical University of Athens, Athens.

Thomann, R.V. and J.A. Mueller (1987), Principles of Surface Water Quality Modeling and Control, HarperCollins, New York.

Upadhayaya A. and H.S. Chauhan (2001), Falling water tables in horizontal/sloping aquifers. Journal of Irrigation and Drainage Engineering 127 (6), pp. 378-385.

Wenneker I., G. Segal and P. Wesseling (2000), Computation of Compressible Flows on Unstructured Staggered Grids. European Congress on Computational Methods in Applied Sciences and Engineering, Barcelona.

Table 1: MODFLOW and 3dkflow maximum errors of simulated hydraulic head and drains discharge.

MODFLOW cells	3dkflow cells	MODFLOW H (m)/Q (m³/s) Max Error	3dkflow H (m)/Q (m³/s) Max Error
10000	150	1.4/0.42	30.4/2.73
2500	73	5.2/2.28	18.7/2.95
400	37	15.1/7.76	22.3/2.85
144	10	28.5/12.48	31.3/3.40
	10*		6.60/3.34

*Note: 3dkflow simulation with 10 parameters.
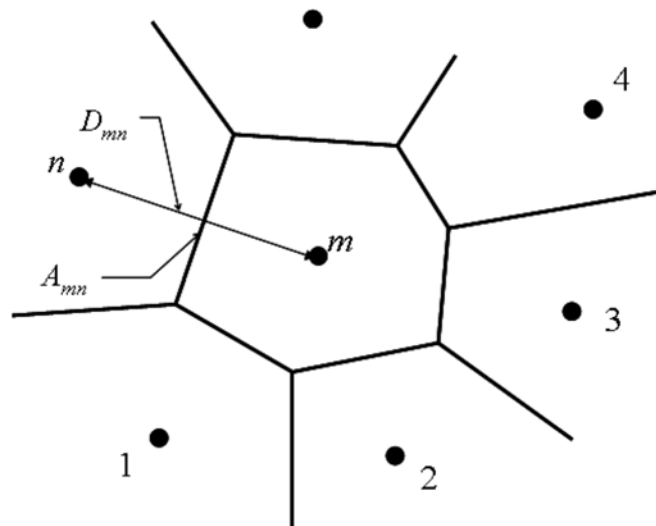
Figure 1: Cell *m* surrounded by *N* neighbouring cells.
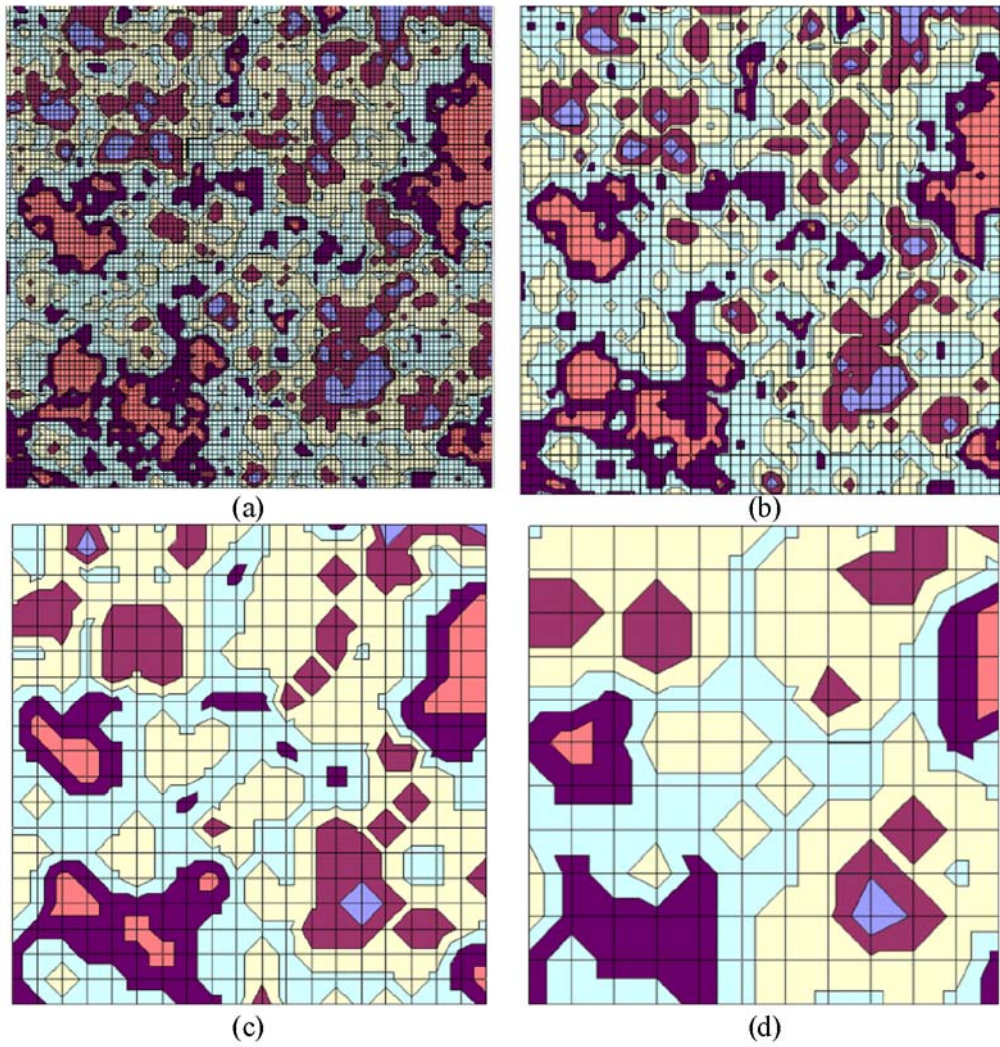
Figure 2: Parameterization of the synthetic aquifer with six zones and discretization of the synthetic aquifer with four FDM grids (100×100, 50×50, 20×20 and 12×12 in panels (a), (b), (c) and (d) respectively).
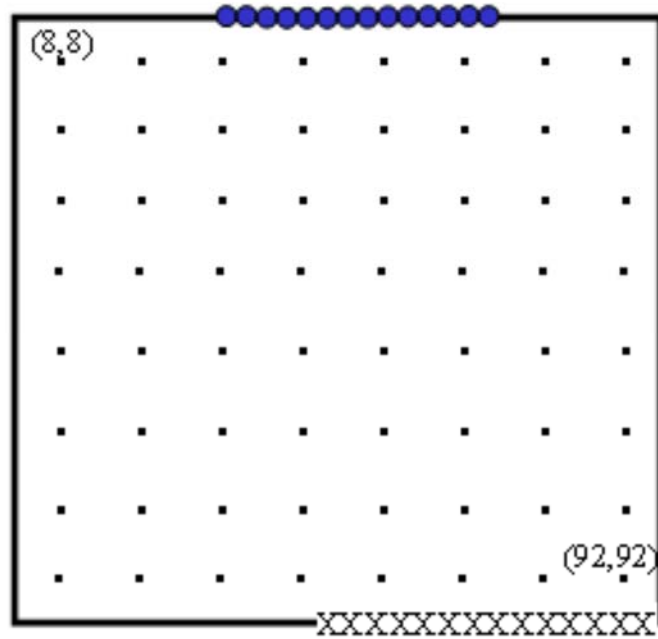
Figure 3: The boundary conditions of the synthetic aquifer (thick lines in the perimeter for no-flow barriers, "×" for the injecting wells and "o" for the drains) and the 8×8 observation grid (observation points marked with "•").
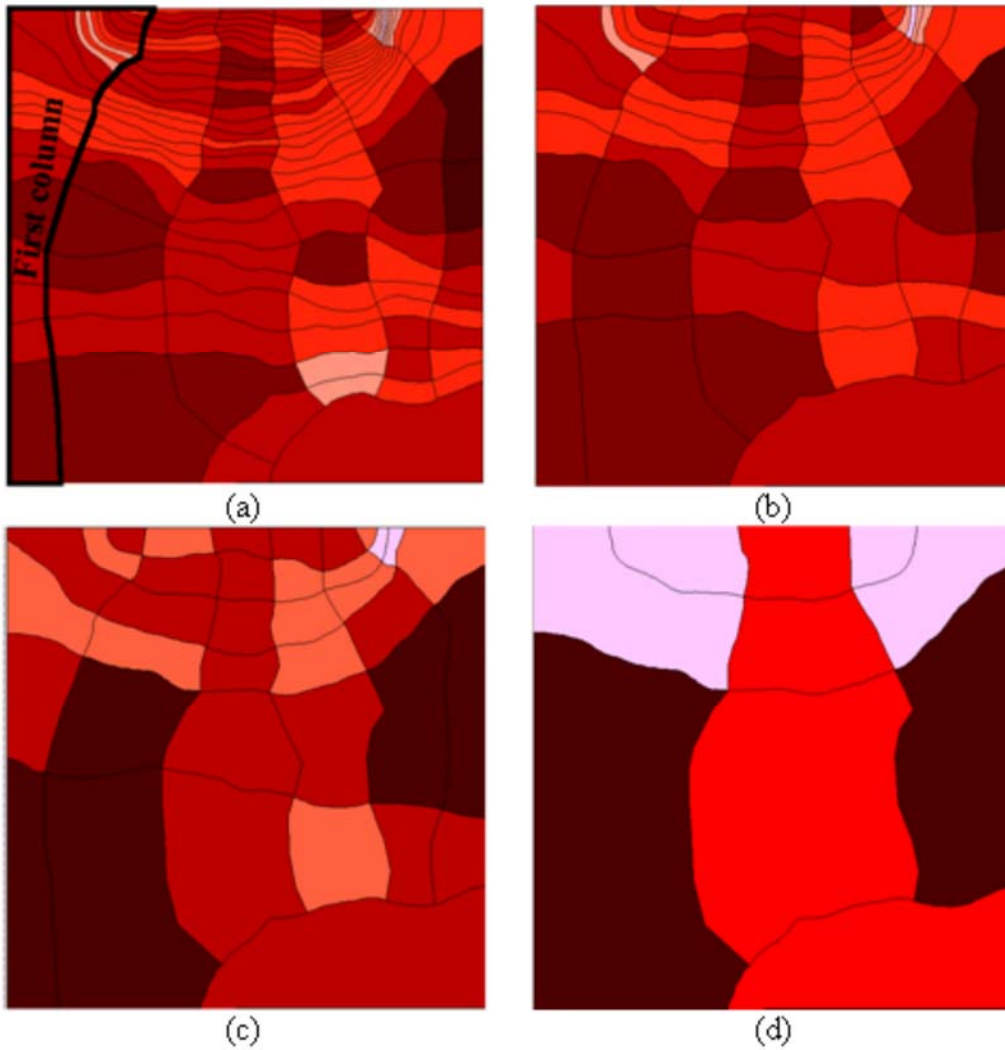
Figure 4: Discretization of the synthetic aquifer with the four FVMSI meshes.
FVMSI meshes with 150, 73, 37 and 10 cells in panels (a), (b), (c) and (d)
respectively. Aquifer parameterization with six zones (panels (a) and (b)), aquifer
parameterization with four zones (panel (c)) and aquifer parameterization with three
zones (panel (d)).
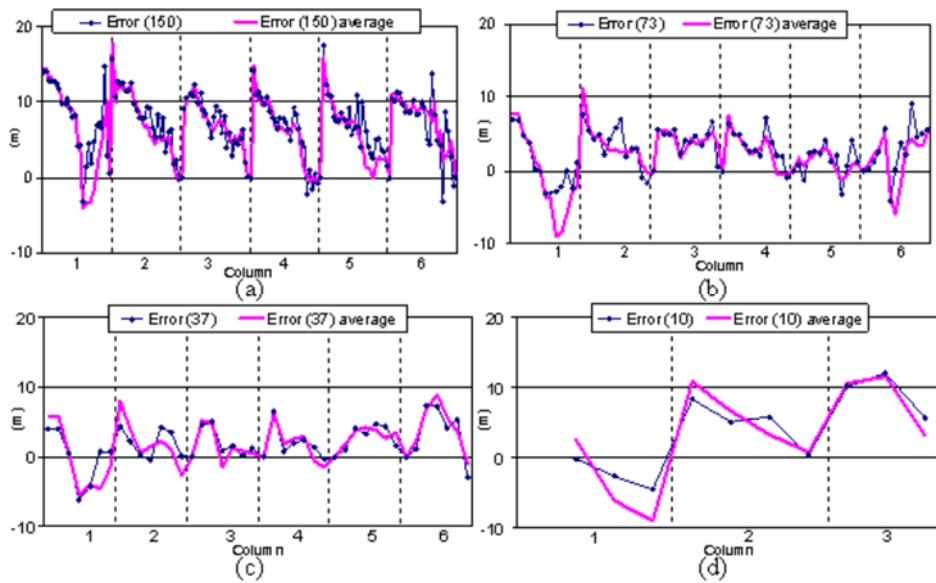
Figure 5: Overall hydraulic head error (deviation from closest cell and from the average value) of the FVMSI meshes with 150,73,37 and 10 cells in panels (a), (b), (c) and (d) respectively (in *x* axis the cell column, see Figure 4a).

$$y = 227.28x^{-0.6725}$$
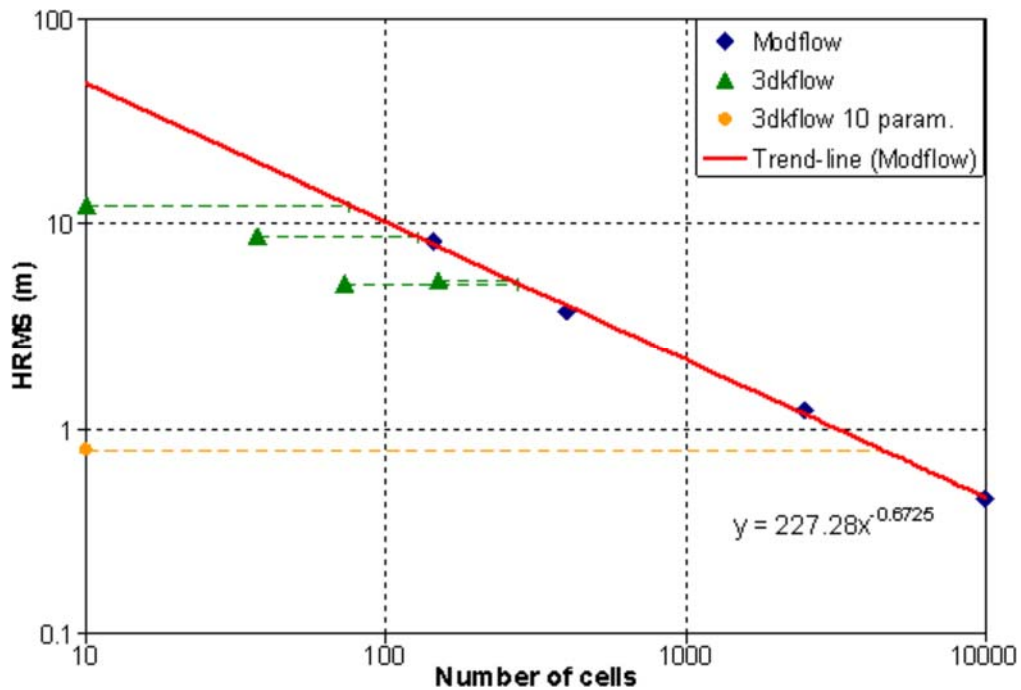
Figure 6: Number of discretisation cells and RMS of the simulated hydraulic head with MODFLOW, with 3dkflow and with 3dkflow with 10 parameters.
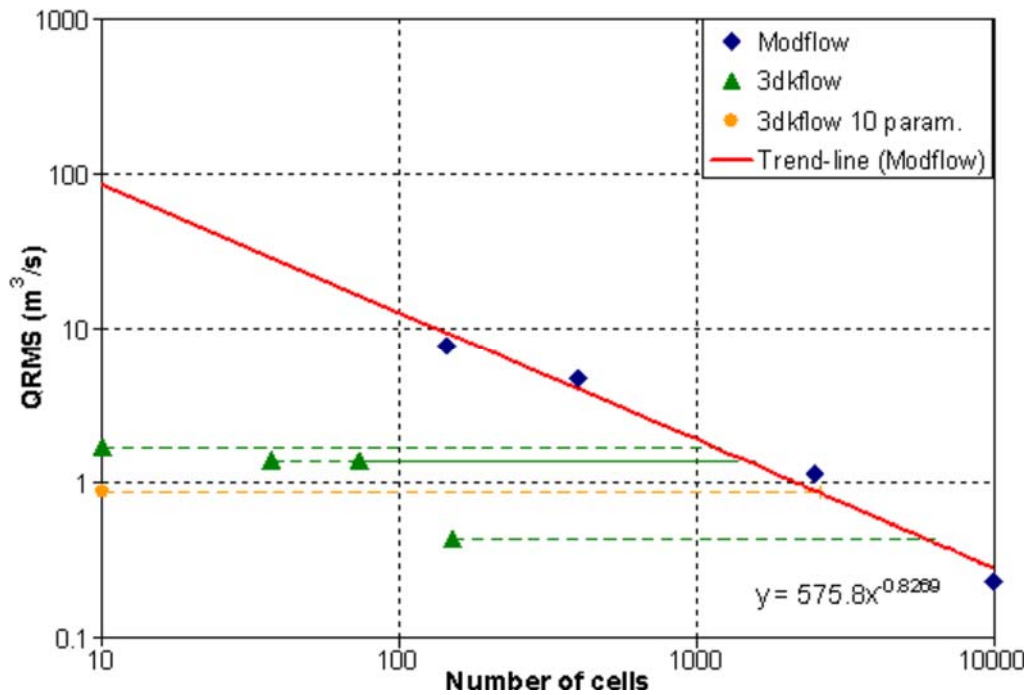
Figure 7: Number of discretisation cells and RMS of the simulated discharge with

MODFLOW, with 3dkflow and with 3dkflow with 10 parameters.
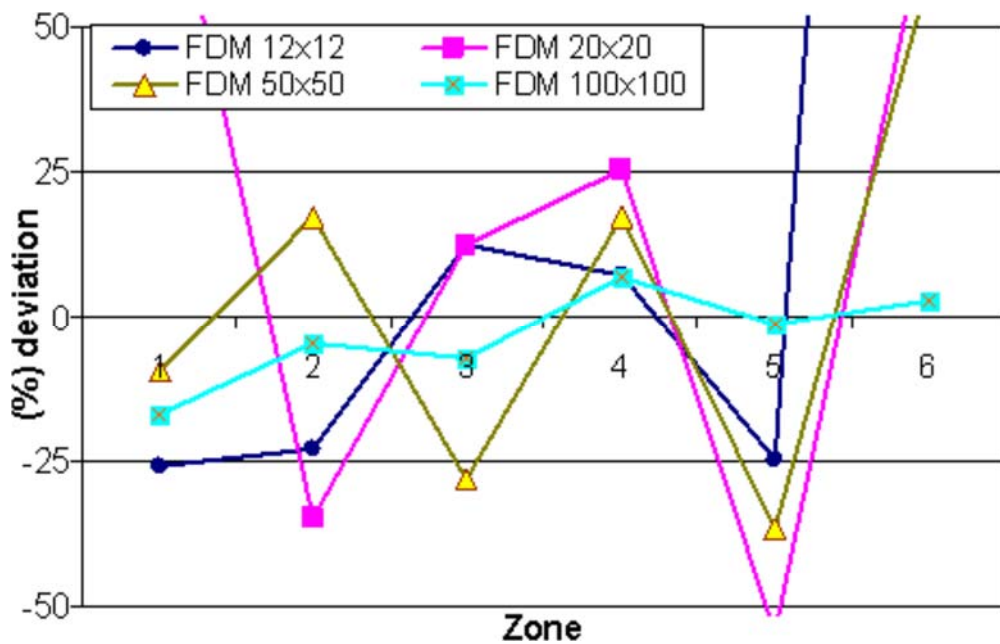
Figure 8: Deviation of the estimated hydraulic conductivities with the four FDM

grids (100×100, 50×50, 20×20 and 12×12) from the reference values.
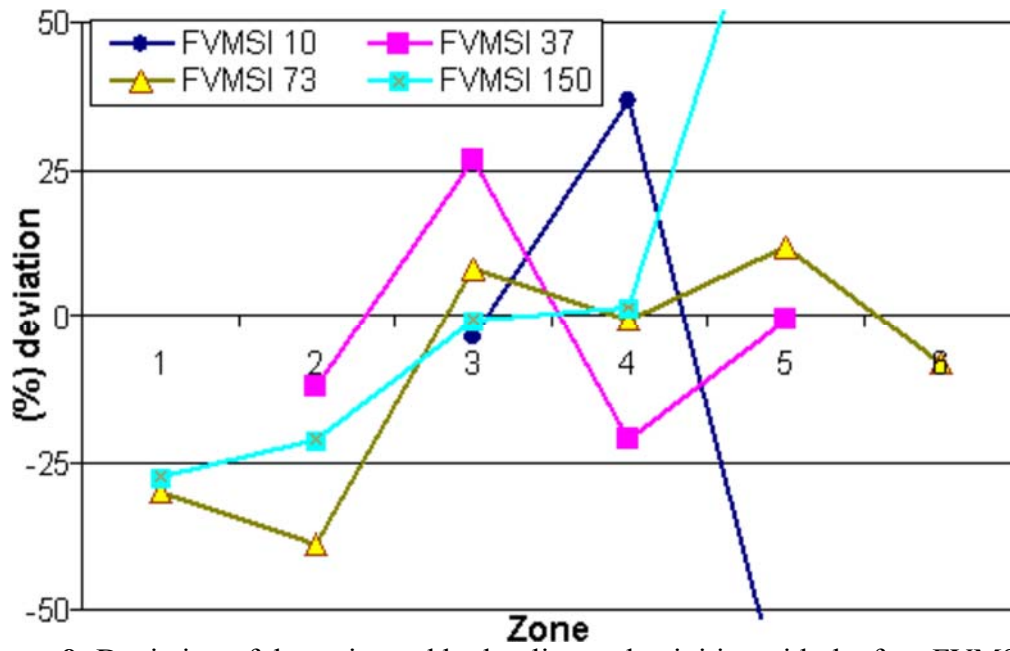
Figure 9: Deviation of the estimated hydraulic conductivities with the four FVMSI

meshes from the reference values.